Ion−Solvent Interactions in Acetonitrile Solutions of Lithium Iodide and Tetrabutylammonium Iodide

Andrew K. Mollner,[†] Paula A. Brooksby,[†] John S. Loring,[‡] Imre Bako,[§] Gabor Palinkas,*[,§] and W. Ronald Fawcett*[,†]

Department of Chemistry, University of California—Davis, Davis, California 95616, Department of Land, Air, and Water Resources, University of California—Davis, Davis, California 95616, and Chemical Research Center, Hungarian Academy of Sciences, Pusztaszeri ut 59/67, H-1025 Budapest, Hungary

Received: October 20, 2003; In Final Form: January 28, 2004

The vibrational spectra of acetonitrile solutions containing lithium iodide and tetrabutylammonium iodide have been studied using ATR-FTIR spectroscopy. The focus of interest was the effect of the iodide anion on the important vibrational bands of acetonitrile. The main effect of the LiI electrolyte is to shift the C≡N stretching frequency in the blue direction due to interaction of the Li^+ cation with the electronegative C≡N group. However, a small red shift of the C≡N stretching mode due to the interaction of I^- with the methyl group of acetonitrile is found in both electrolytes. On the other hand, the symmetic and asymmetric stretching modes of the methyl group are significantly red shifted in the presence of LiI. Ab initio quantum chemical calculations were carried out to determine the optimum location of the Li^+ and I^- ions in ion−solvent complexes containing a varying number of solvent molecules. These calculations correctly predict the direction of the observed shifts for all the principal bands of acetonitrile except the methyl stretching modes.

Introduction

Vibrational spectroscopy is a very useful tool for studying ion−solvent interactions in electrolyte solutions.[1] In the case of aprotic solvents such as acetonitrile, dimethyl sulfoxide, and acetone, FTIR spectroscopy is the most convenient method especially when it is used in the attenuated total reflection (ATR) mode. In previous work, ATR-FTIR spectroscopy was used to study ion−solvent and ion−ion interactions in a variety of perchlorate solutions in acetonitrile; these included the alkali metal perchlorates,[2] the alkaline earth metal perchlorates,[3,4] and other divalent metal perchlorates.[3] The analysis of the spectroscopic data was significantly improved recently[5] by carefully considering the correction of ATR data for distortion due to varying effective path length, and by applying factor analysis[6] to spectral data obtained as a function of electrolyte concentration. When data for acetonitrile solutions containing $LiClO_4$, $NaClO_4$, and tetraethylammonium perchlorate were examined,[7] it was shown that the C≡N stretching frequency is affected not only by the nature of the cation of the electrolyte but also by the anion. Although the latter effect is subtle, its recognition was a major step forward in the interpretation of electrolyte effects on the solvent's vibrational properties in these systems.

In the present paper, a detailed study of the FTIR spectra of acetonitrile solutions of LiI is reported. By changing the anion of the electrolyte from perchlorate to iodide, it was anticipated that a more careful examination of the anion's role in spectral features would be possible. Experiments were also carried out in tetrabutylammonium iodide (TBAI). In this way, the role of the small Li^+ in determining spectral features could be more carefully assessed by comparison with spectra obtained in the presence of the large TBA^+ cation. Ab initio quantum mechanical calculations were carried out to describe the important features of the IR spectrum. By using an electrolyte with monatomic ions, the number of atoms associated with an ion−solvent cluster was kept at a minimum. The initial results of these calculations are also presented in this paper and compared with the experimental spectroscopic data.

Experimental Methods

Anhydrous acetonitrile (AcN) (99.8% < 0.005% water) was purchased from Aldrich and was not purified further. LiI (Sigma, 99%) and TBAI (Aldrich) were dried in the dark and under vacuum at 140 °C for 24 h. Manipulations of the salts and acetonitrile were done inside a nitrogen filled glovebox. All solutions were prepared by weight. A 20 cm^3 pycnometer (calibrated with water at 25 °C) was used to calculate the densities of a series of five electrolyte solutions in AcN with known weights. These calibration curves were used to convert the sample solution weights to molarity.

A Mattson Galaxy 3000 RS-1 spectrometer was used for all infrared measurements. The spectrometer was operated at ambient pressures in an environment that had been purged significantly free of CO_2 and atmospheric water (PUREGAS Air Dryer, model CDA 1120). The spectrometer was equipped with a Ge/KBr beam splitter, a mechanical interferometer having cubic mirrors, a water cooled Globar ceramic source, and a DTGS detector operating at room temperature. A custom built overhead ATR cell (University of California, Davis) was designed to fit into the sample compartment of the Mattson spectrometer; it permitted use of a trapezoidal CdTe internal reflection element (Spectral Systems, 45° and 50 × 20 × 3 mm). All pATR spectra were obtained using a resolution of 1 cm^{-1} and analyzed by taking the negative logarithm of the ratio of sample and background single beam spectra. The empty ATR

* To whom correspondence should be addressed. E-mail: palg@chemres.hu (G.P.); wrfawcett@ ucdavis.edu (W.R.F.).
† Department of Chemistry, University of California, Davis.
‡ Department of Land, Air, and Water Resources, University of California, Davis.
§ Hungarian Academy of Sciences.

10.1021/jp037174y CCC: $27.50
Published on Web 03/30/2004

cell blanketed with argon gas was used to collect the background spectrum. The cell was shown[5] to have an angle of incidence of 49.4° and 6.2 reflections. Distortions in the sample pATR spectra due to dispersion effects were found to be minor; as a result, it was not necessary to convert to linear absorbance spectra.

LinkFit[5,6] was used to perform single-dimensional spectral curve fits. Lorentzian, Gaussian, or mixed Lorentzian−Gaussian curves were fitted to spectral bands via the Levenberg−Marquardt algorithm. Polynomial baselines were fitted during the nonlinear least squares iteration, or they were calculated and subtracted from the spectrum prior to the curvefit. Multiple dimensional curvefits[6] were also performed using a factor analysis routine.[5−7] The pATR spectra collected as a function of known solution concentrations were organized into a matrix, **A**, where the columns represented the individual pATR spectra and the rows are the pATR values at the wavenumbers used in the analysis. This matrix is factored into two additional matrices, $\mathbf{A} = \mathbf{BP}$, where the columns of **B** are the basis spectra comprising the pATR spectra in **A**, and the rows, **P**, give the contributions of the basis spectra to the corresponding pATR spectrum. The elements of **P** may be mathematically modeled based upon knowledge of the components of the system, stoichiometry, concentrations, pH, and so forth. However, the large sizes of the matrixes created are conveniently simplified by using a numerical analysis routine called singular value decomposition (SVD). SVD factors **A** into smaller matrixes that are more reasonable for transforming the SVD output into **B** and **P**. Furthermore, the SVD output allows the determination of the number of significant basis spectra. If there is no prior knowledge of the basis spectra, this provides an important advantage. The significance of the basis spectra was evaluated numerically using its percent of the total variance. A basis spectrum was considered insignificant if it accounted for less than 0.01% of variance. The spectra with percent of variance below 0.01 were attributed to noise and baseline drift. A detailed description of all of the software used in this analysis has been published elsewhere.[5]

Quantum Calculations

The structure of ion−solvent complexes, namely, $[Li(AcN)_n]^+$ where $n = 1-4$, and $[I(AcN)_n]^-$ where $n = 1$ or 2 was studied by ab initio quantum calculations. Each structure was optimized by searching for a minimum in its potential hypersurface using the Gaussian 98 program package with the MP2 method and the SDD basis set.[8] The SDD basis set contains the valence double ζ D95V basis set for the elements in the first row, and the Stuttgart−Dresden effective pseudopotentials for heavier atoms. Since the I^- ion contains a large number of core electrons, the relativistic effect is important and the all electron calculation is subject to error.[9]

The intermolecular interaction energy for each cluster was calculated by the supermolecule method using the counter poise (CP) correction[10] in order to avoid the basis set superposition error. The charge distribution and charge-transfer processes were investigated by the natural bond order (NBO) method. The calculated harmonic frequencies for the clusters were not scaled.

Results and Discussion

Infrared Spectra. ATR-FTIR spectra were obtained for pure acetonitrile (AcN) and for solutions of LiI and TBAI in AcN. Spectra were measured for five precisely known concentrations in the range from 0.1 to 0.8 M. The analysis of the spectral data was carried out using the procedure described in a previous paper.[5] The spectrum of pure AcN as well as the effects of alkali metal cations are well-known.[2] The focus of interest here is the effect of a monatomic anion, namely iodide, on the spectral properties of AcN.

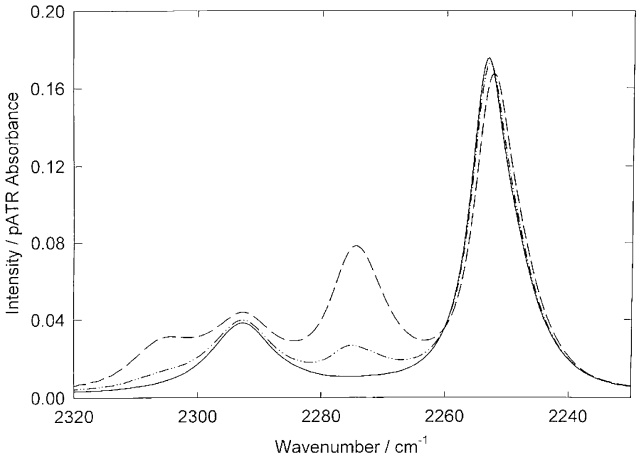

Figure 1. Infrared spectra for pure AcN (—) and two solutions of LiI in AcN (0.16 (-···-) and 0.77 M (- - -) in the C≡N stretch region (2230−2320 cm^{-1}).

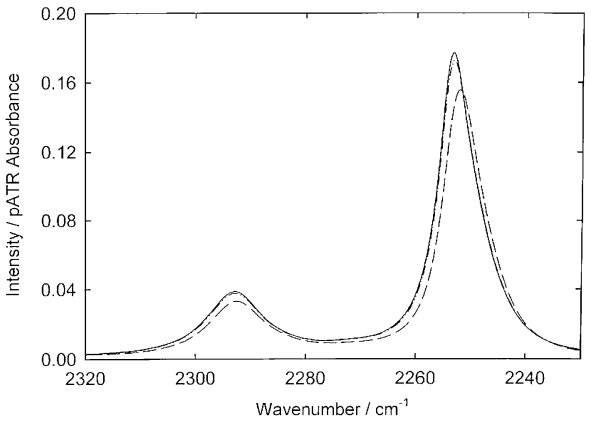

Figure 2. Infrared spectra for pure AcN (—) and two solutions of TBAI in AcN (0.06 (-···-) and 0.73 M (- - -) in the C≡N stretch region (2230−2320 cm^{-1}).

The spectra of two LiI solutions are compared with that of pure AcN for the 2230−2320 cm^{-1} region in Figure 1. The C≡N stretching frequency (ν_2) is seen at 2253 cm^{-1} and the combination band ($\nu_3 + \nu_4$) at 2293 cm^{-1} in pure acetonitrile. In the presence of LiI, two new bands appear at 2275 and 2306 cm^{-1}, which are attributed to a Li^+···AcN complex. The first of these is due to the C≡N stretch, and the second, to the combination band. It is also apparent that the ν_2 band at 2253 cm^{-1} is shifted to lower frequencies with increase in electrolyte concentration. This is attributed to the interaction of the I^- anion with the AcN molecule. The corresponding data for the TBAI system are shown in Figure 2. Because of its large size and shielded charge, the TBA^+ cation does not affect the vibrational properties of AcN in a significant way. On the other hand there is a clear effect on both the ν_2 band and the $\nu_3 + \nu_4$ combination band from the iodide anion.

When factor analysis is performed on the spectral data, two basis spectra are found. The first corresponds to unperturbed AcN and is exactly the same as the spectrum of pure AcN. The second spectrum is that of AcN molecules associated with ions. The results for the LiI and TBAI systems are shown in Figures 3 and 4, respectively. Four bands are apparent in the spectrum of associated AcN. Those attributed to the Li^+ complexes are

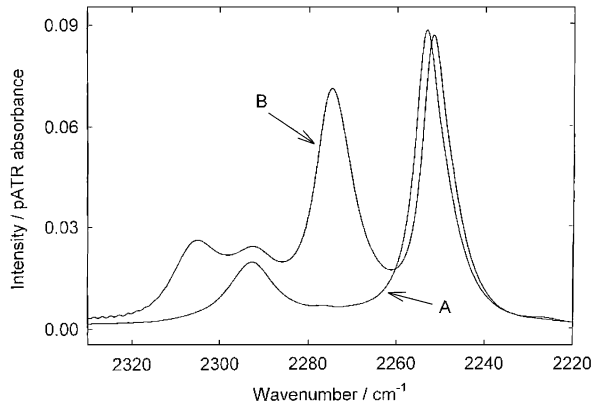

Figure 3. Infrared spectrum shown in Figure 1 for the 0.77 M LiI solution in AcN after factor analysis. Spectrum A corresponds to the spectrum of pure AcN, and spectrum B, to that of AcN interacting with Li^+ and I^- ions.

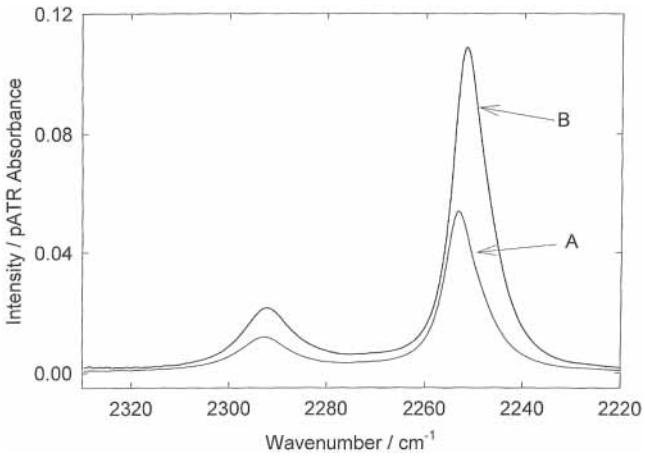

Figure 4. Infrared spectrum shown in Figure 2 for the 0.73 M TBAI solution in AcN after factor analysis. Spectrum A corresponds to the spectrum of pure AcN, and spectrum B, to that of AcN interacting with TBA^+ and I^- ions.

at 2275 and 2306 cm^{-1} exactly as seen in the spectra for the LiI solutions (Figure 1). The bands at 2252 and 2292 cm^{-1} are attributed to the $I^-\cdots$AcN complex. These correspond to the C≡N stretch and the combination band, respectively. Keeping in mind the fact that the I^- anion interacts with the positive end of the AcN molecular dipole, that is, with the methyl group, this effect is transmitted through the C−C bond and therefore is weak in comparison to the cation interaction. Nevertheless, it cannot be ignored in interpreting the spectral data. The analysis of the data for the LiI solutions is confirmed with the basis spectra for the TBAI solutions (Figure 4). The spectrum for associated AcN molecules shows two bands in the same positions as those bands attributed to the $I^-\cdots$AcN complex in the LiI solution. Both bands are slightly red shifted with respect to the corresponding bands in pure AcN.

Spectral data for pure AcN and LiI−AcN solutions in the region from 2850 to 3050 cm^{-1} are shown in Figure 5. Two peaks are seen in the spectrum of pure AcN at 2944 and 3004 cm^{-1}, corresponding to the symmetrical stretch (ν_5) and asymmetrical stretch (ν_1) of the CH_3 group, respectively. In the LiI solution, at least two additional bands appear at 2926 and 2980 cm^{-1}. These are attributed to the effects of interaction of the I^- anion with the symmetrical and asymmetrical stretching modes of the CH_3 group, respectively. After performing factor analysis on the spectra in this region, a clearer picture of the effects of ion−solvent interactions emerges (Figure 6). Thus,

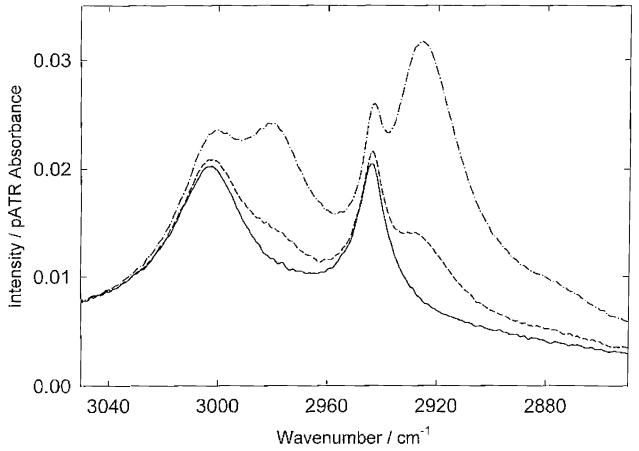

Figure 5. Infrared spectra for pure AcN and two solutions of LiI in AcN (0.16 and 0.77 M) in the C−H stretch region (2850−3050 cm^{-1}).

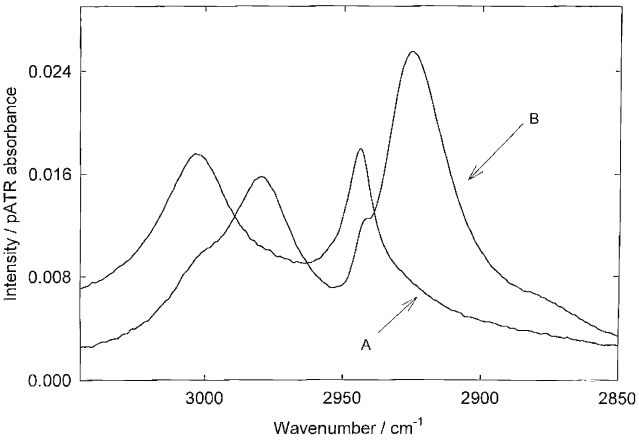

Figure 6. Infrared spectrum shown in Figure 5 for the 0.77 M LiI solution in AcN after factor analysis. Spectrum A corresponds to the spectrum of pure AcN, and spectrum B, to that of AcN interacting with Li^+ and I^- ions.

the spectrum for associated AcN molecules shows bands at 2926 and 2980 cm^{-1} with shoulders at 2943 and 3002 cm^{-1}, respectively. The shoulders are attributed to interaction of the Li^+ cation at the negative end of the molecular dipole with the CH_3 vibrational modes. The effect is weak, corresponding to a red shift of the order of 1 cm^{-1}, because it is transmitted through both the C≡N and C−C bonds to the methyl group. Spectral data for the TBAI system in this region are not presented. These spectra are complicated due to the contribution of the butyl group to absorption in this region. Therefore, they do not shed further light on the interaction of AcN with monatomic ions.

Spectral data in the 890−950 cm^{-1} range and the 700−820 cm^{-1} range are shown for the LiI system in Figure 7. The band at 918 cm^{-1} in pure AcN corresponds to the C−C stretch (ν_4) and that at 748 cm^{-1} to the C−C≡N bending mode ($2\nu_8$). New bands at higher frequencies are seen for the LiI solutions. These are attributed to $Li^+\cdots$AcN complexes. After factor analysis, a small effect of the $I^-\cdots$AcN complexes can be seen in the bands which are closest to the bands in pure AcN (see Figure 8). In the case of the C−C stretch, the band in the spectrum for the associated solvent molecules is shifted by a very small amount to lower frequencies, whereas for the bending mode, it is shifted slightly to higher frequencies.

In summary, these experiments have shown a clear contribution of the anion to the infrared spectral features observed in LiI and TBAI solutions in AcN. The anion effect is stronger than that found earlier for perchlorate solutions.[5] This is simply

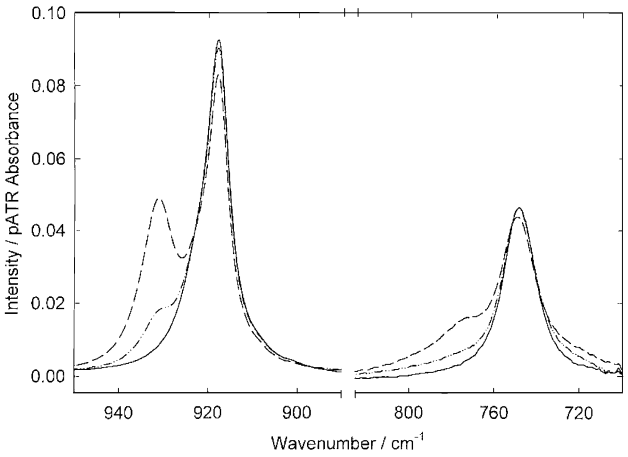

Figure 7. Infrared spectra for pure AcN and two solutions of LiI in AcN (0.16 and 0.77 M) in the C−C stretch region (890 to 950 cm^{-1}) and the C−C≡N bending region (700−820 cm^{-1}).

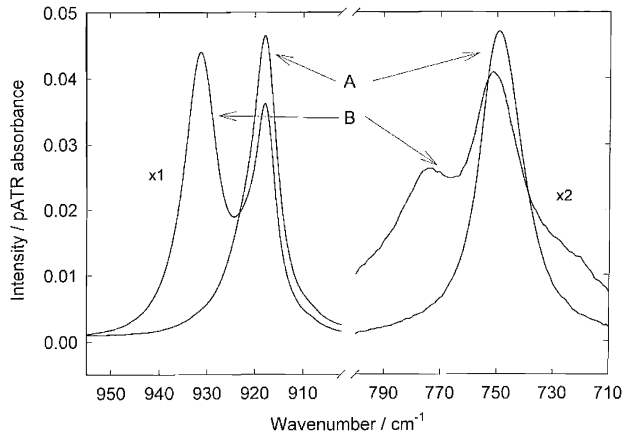

Figure 8. Infrared spectrum shown in Figure 7 for the 0.77 M LiI solution in AcN after factor analysis. Spectrum A corresponds to the spectrum of pure AcN, and spectrum B, to that of AcN interacting with Li^+ and I^- ions.

due to the fact that the field due to iodide is larger than that due to perchlorate considering both the charge distribution in and size of the polyatomic ClO_4^- ion.

Ab Initio Quantum Chemical Calculations. The properties of $Li(AcN)_n$ clusters were estimated as described above for the cases that $n = 1-4$. As one would expect, the optimum geometry of the complex was linear for the case of two ligands around Li^+, trigonal for $n = 3$, and tetrahedral for $n = 4$. The bonding between Li^+ and AcN was always through the nitrogen atom at the negative end of the AcN molecular dipole. The geometry of the complex for $n = 4$ is shown in Figure 9, and some of the estimated properties are summarized in Table 1. The stabilization of the Li^+ ion is reflected by the value of ΔE, the interaction energy, which increases in magnitude with the number of AcN molecules up to four. When a calculation was performed with five AcN molecules, the optimum location for the fifth molecule was in the second solvation layer. Thus, it is concluded that the optimum solvation number for Li^+ in AcN is four in the absence of contact ion pairing. The Li^+−N distance in the complex increases from 194 pm with one AcN molecule in the complex to 205 pm when there are four ligands. Only small changes are seen in the internal bond distances in the solvent molecule when it is a ligand. These have their largest values when only one ligand is involved; thus, the C≡N bond decreases in length by 1.3 pm and the C−C bond by 0.5 pm in the complex $Li(AcN)^+$ These results are in agreement with

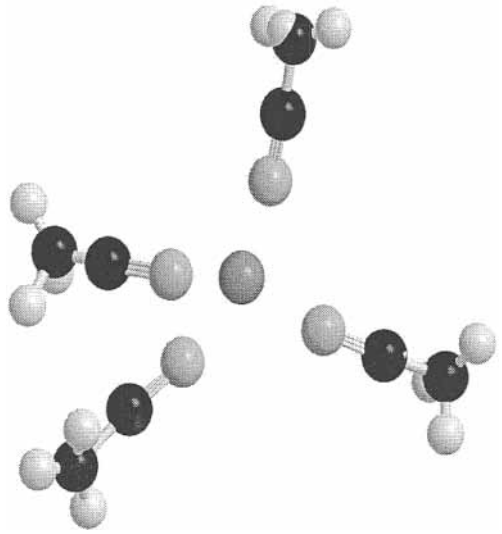

Figure 9. Optimum geometry for a complex consisting of a central Li^+ ion with four surrounding acetonitrile molecules.

TABLE 1: Selected Properties of $Li^+\cdots$AcN Complexes Calculated by the mp2/SDD Method

		bond length/pm		
complex	ΔE/kJ mol^{-1}	Li−N	C≡N	C−C
AcN			121	149
$Li(AcN)^+$	−177	194	120	149
$Li(AcN)_2^+$	−330	196	120	149
$Li(AcN)_3^+$	−431	199	120	149
$Li(AcN)_4^+$	−498	205	120	149

TABLE 2: Estimated Vibrational Frequencies for $Li^+\cdots$AcN Complexes

	frequency of band[a]/cm^{-1}			
complex	$2\nu_8$	ν_4	ν_2	$\nu_3+\nu_4$
AcN	347	892	2063	2366
$Li(AcN)^+$	391	921	2165	2394
	(44)	(29)	(102)	(28)
$Li(AcN)_2^+$	386	913	2162	2387
	(39)	(20)	(99)	(21)
$Li(AcN)_3^+$	393	910	2145	2385
	(46)	(18)	(85)	(19)
$Li(AcN)_4^+$	394	908	2137	2384
	(47)	(16)	(77)	(18)

[a] The numbers in brackets give the estimated frequency shift for the complex with respect to unperturbed AcN.

earlier calculations in which the Hartree−Fock and density functional theory (DFT/B31YP) methods were used.[11,12]

Calculated freequencies for the $\nu_3 + \nu_4$, ν_2, ν_4, and $2\nu_8$ bands in pure AcN and for $Li^+\cdots$AcN complexes are summarized in Table 2. The most important result of these calculations is that a blue shift is estimated for all of these bands as a result of the interaction of the AcN molecule with the Li^+ ion. Furthermore, the blue shift is due to charge transfer from the lone pair on the nitrogen atom of AcN to the Li^+ ion. The loss of electron density associated with the lone pair results in an increase in the strength of the C≡N bond and an increase in its frequency. This effect is transmitted throughout the molecule so that blue shifts are also seen for the $\nu_3 + \nu_4$ combination band and the ν_4 and $2\nu_8$ bands. The magnitudes of the estimated shifts are too large in comparison with experiment. By choosing a more flexible basis set for the quantum chemical calculations, better estimates of these quantities could be made. Finally, the value of the frequency shift decreases with increase in the number of ligands, that is, with change in the electrostatic environment in the

TABLE 3: Natural Bond Order Analysis for the $Li(AcN)_n^+$ Complexes

charge/e	AcN	$Li(AcN)^+$	$Li(AcN)_2^+$	$Li(AcN)_3^+$	$Li(AcN)_4^+$
H	0.245	0.271	0.262	0.253	0.257
C_1	−0.675	−0.690	−0.688	−0.684	−0.680
C_2	0.358	0.590	0.561	0.519	0.460
N	−0.417	−0.714	−0.659	−0.594	−0.550
Li^+		0.990	0.950	0.900	0.870
N_{LP}	1.973	1.970	1.955	1.940	1.900
Li_{LP}	0.009	0.045	0.094	0.140	
energy/ kJ mol^{-1}					
$\Delta E_{2,Li}$		17.4	57.7	89.5	113.8
$\Delta E_{2,C-C}$	56.3	45.6	44.8	45.6	52.3

TABLE 4: Selected Properties of the $I^-\cdots$AcN Complexes Calculated by the mp2/SDD Method

		bond length/pm			
complex	ΔE/kJ mol^{-1}	I−C	C−H	C−C	C−N
$I(AcN)^-$	−37.2	383	110	149	121
$I(AcN)_2^-$	−71.5	386	110	143	121

complex to one more characteristic of the real environment for AcN within the complex.

The third aspect of the quantum chemical calculations performed here was a natural bond orbital analysis[9] to determine the charge distribution within the AcN molecules in the clusters. The results for Li^+ are given in Table 3. The largest change in charge is associated with the C and N atoms of the C≡N group when they are in clusters. In effect, the dipole moment of the C≡N system increases as a result of the charge-transfer processes which accompany cluster formation. On the other hand, the charge on the carbon and hydrogen atoms of the methyl group change very little when a Li^+ complex is formed. The charge associated with the lone pair on the nitrogen atom in AcN is 1.97 electrons in the unperturbed molecule. In the $Li^+\cdots$AcN complexes, this charge drops from 1.97 electrons to 1.90 as the number of AcN ligands increases from 1 to 4. At the same time, the charge associated with the antibonding lone pair orbital increases from 0.01 to 0.14 electron. The last quantities recorded in Table 3 are the estimates of the second-order perturbation energies ΔE_2 of the "donor-acceptor" interactions between the N lone pair and Li^+ ($\Delta E_{2,Li^+}$), and between the N lone pair and the antibonding orbital associated with the C−C bond ($\Delta E_{2,C-C}$). $\Delta E_{2,Li^+}$ increases markedly with the number of AcN molecules in the complex; on the other hand, $\Delta E_{2,C-C}$ increases very slightly with the same change.

The properties of $I^-\cdots$AcN clusters were estimated for the cases of 1 or 2 AcN molecules in the complex, and are shown in Table 4. The $I(AcN)^-$ system has C_{3v} symmetry with the I^- ion bound directly to the carbon atom of the methyl group in AcN. On the other hand, $I(AcN)_2^-$ has a linear structure with an angle very close to 180° for the C−I−C bond formed between the carbon atoms in the two methyl groups, one on each AcN molecule, and the I atom (see Figure 10). In the dimer, the I−C distance is about 2.5 pm longer than in the cluster with one AcN molecule. The C−H bond distances are slightly smaller and the C−C and C≡N distances slightly larger in the clusters. There are no bent structures in which one hydrogen atom in the methyl group is closer to the I atom than the other two H atoms. On the other hand, complexes with a bent structure were found in the case of $Br^-\cdots$AcN clusters.[13] Another result is that the potential energy surface around the methyl group is extremely flat. As a final remark, it should be noted that calculations were limited to the case of 1 or 2 AcN molecules in the cluster simply because the number of electrons in the system becomes very large with more solvent molecules.

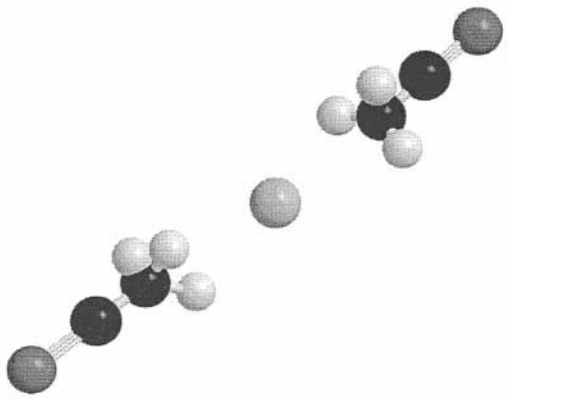

Figure 10. Optimum geometry for a complex consisting of a central I^- ion with two surrounding acetonitrile molecules.

TABLE 5: Estimated Vibrational Frequencies for $I^-\cdots$AcN Complexes

	frequency of band/cm^{-1}			
complex	ν_4	ν_2	ν_5	ν_1
AcN	892	2063	3047	3156
$I(AcN)^-$	875	2054	3069	3180
	(−17)	(−9)	(22)	(24)
$I(AcN)_2^-$	877	2056	3068	3178
	(−15)	(−7)	(21)	(22)

TABLE 6: Natural Bond Order Analysis for the $I(AcN)_n^-$ Complexes

charge/e	AcN	$I(AcN)^-$	$I(AcN)_2^-$
H	0.245	0.262	0.260
C_1	−0.675	−0.695	−0.690
C_2	0.358	0.387	0.384
N	−0.417	−0.491	−0.491
I		−0.981	−0.988
I_{LP}		1.989	1.973
energy/kJ mol^{-1}			
$\Delta E_{2,C-C}$		10.3	6.3

Calculated frequencies for the C≡N (ν_2) and C−C (ν_4) stretching modes and the symmetical (ν_1) and asymmetrical (ν_5) CH_3 stretching modes in the $I^-\cdots$AcN complexes are compared with the experimental results in Table 5. The ν_2 and ν_4 bands are shifted in the red direction in agreement with experimental observation. On the other hand, the modes associated with the CH_3 group (ν_1 and ν_5) are blue shifted, whereas the bands observed experimentally are red shifted. The calculated results can be attributed to charge transfer from a lone pair on the iodide ion to the antibonding orbital associated with the C−C bond. It follows that the C−C bond is made slightly weaker. This effect is reflected in the adjacent bonds with the result that the C≡N bond is also slightly weaker, but the CH bonds in the methyl group become significantly stronger.[14]

Results of the natural bond order analysis for the $I^-\cdots$AcN complexes are summarized in Table 6. Significant changes are found in the charges associated with the methyl group carbon and hydrogen atoms and with the carbon and nitrogen atoms of the CN group. The estimates of the second-order perturbation energy of the donor−acceptor interaction between the I^- ion and the antibonding orbital on the C−C bond decreases significantly with the number of I^- ligands.

The quantum chemical estimates of the frequencies of the important infrared bands for AcN are compared with the experimental data in Table 7. In the case of the ν_2, ν_4, and 2 ν_8

TABLE 7: Experimental and Estimated Vibrational Frequencies in cm^{-1}[a]

system	CH_3 stretch, symmetrical ν_5	CH_3 stretch, asymmetrical ν_1	combination band $\nu_3 + \nu_4$	C≡N stretch ν_2	C−C stretch ν_4	C−C≡N bend ν_8
			Experiment			
pure AcN	2944	3004	2293	2253	918	748
AcN interacting						
with Li^+	2943 (−1)	3002 (−2)	2306 (13)	2275 (22)	932 (26)	774 (26)
with I^-	2926 (−18)	2980 (−24)	2292 (−1)	2252 (−1)	915 (−3)	749 (1)
			Theory			
pure AcN	3047	3156	2363	2063	892	694
AcN interacting						
with Li^+	3050 (3)	3159 (3)	2384 (21)	2137 (74)	908 (16)	788 (94)
with I^-	3068 (21)	3178 (22)		2056 (−7)	877 (−15)	

[a] The numbers in brackets show the shift in the band due to interaction with the given ion.

bands and the $\nu_3 + \nu_4$ combination band, theory correctly predicts the direction of the shifts due to the interaction of AcN with the ions. However, the estimated magnitude is usually too large. Improvement of the basis set should result in better quantitative agreement between theory and experiment. In the case of the CH_3 stretching frequencies, the predicted shift due to I^- is in the opposite direction to the red shift observed experimentally. This may be due to the fact that the present results are based on an AcN dimer. In fact, approximately eight AcN molecules surround the I^- ion, so that the theoretical result could be quite different if calculations for a more realistic complex could be carried out. The differences between the predicted and experimental shifts for these bands due to Li^+ are not considered to be significant.

Concluding Remarks

The effect of cations on the infrared spectrum of AcN is well-known.[2−5] The present data confirm the conclusions reached in a study of the effect of alkali metal perchlorates on the spectrum of AcN. In addition, the quantum chemical calculations show that the Li^+ cation causes a blue shift of the C≡N stretching frequency, the C−C stretching frequency and the C−C≡N bending frequency in agreement with the experimental results. The effect of the anion, which is much less well-known, is clearly seen at several points in the spectra especially after the data have been deconvoluted to give the underlying basis spectra. Interaction of the anion with AcN occurs at the positive end of the molecular dipole, that is with the methyl group. The largest effect of the anion is to shift the symmetrical and asymmetrical CH_3 vibrations in the blue direction. In addition, there is a small but important shift of the C≡N band in the red direction. As a result previous estimates of ion pairing constants[2−4] based on the decrease in intensity of this band with the increase in electrolyte concentration may be in error. The natural bond order analysis obtained from the quantum chemical calculations is especially helpful in understanding the changes in the spectral features that are observed when the electrolyte is added to AcN.

Acknowledgment. This research was carried out under the U.S.−Hungary Joint Research Program with support from the National Science Foundation, Washington (NSF INT-9907943) and the Hungarian Academy of Sciences (MTA-NSF 018/2000). Additional support came to W.R.F. from NSF (CHE-9729314 and CHE-0133758) and to I.B. as a Bolyai stipend from the Hungarian Academy of Sciences.

References and Notes

(1) *The Chemical Physics of Solvation, Part B, Spectroscopy Solvation*; Dogonadze, R. R., Kalman, E., Kornyshev A. A., Ulstrup, J., Eds.; Elsevier: Amsterdam, 1986.

(2) Fawcett, W. R.; Liu, G.; Faguy, P. W.; Foss, C. A. Jr.; Motheo, A. J. *J. Chem. Soc., Faraday Trans*. **1993**, *89*, 811.

(3) Fawcett, W. R.; Liu, G. *J. Phys. Chem*. **1992**, *96*, 4231.

(4) Fawcett, W. R.; Liu, G.; Kloss, A. A. *J. Chem. Soc., Faraday. Trans*. **1994**, *90*, 2697.

(5) Loring, J. S.; Fawcett, W. R. *J. Phys. Chem. A* **1999**, *103*, 3608.

(6) Loring, J. S., Doctoral Dissertation, University of California, Davis, 1999.

(7) Malinowski, E. R. *Factor Analysis in Chemistry*, 2nd ed.; Wiley: New York, 1991.

(8) Frisch, M. J.; Trucks, G. W.; Schlegel, H. B.; Scuseria, G. E.; Robb, M. A.; Cheeseman, J. R.; Zakrzewski, V. G.; Montgomery, J. A., Jr.; Stratmann, R. E.; Burant, J. C.; Dapprich, S.; Millam, J. M.; Daniels, A. D.; Kudin, K. N.; Strain, M. C.; Farkas, O.; Tomasi, J.; Barone, V.; Cossi, M.; Cammi, R.; Mennucci, B.; Pomelli, C.; Adamo, C.; Clifford, S.; Ochterski, J.; Petersson, G. A.; Ayala, P. Y.; Cui, Q.; Morokuma, K.; Malick, D. K.; Rabuck, A. D.; Raghavachari, K.; Foresman, J. B.; Cioslowski, J.; Ortiz, J. V.; Stefanov, B. B.; Liu, G.; Liashenko, A.; Piskorz, P.; Komaromi, I.; Gomperts, R.; Martin, R. L.; Fox, D. J.; Keith, T.; Al-Laham, M. A.; Peng, C. Y.; Nanayakkara, A.; Gonzalez, C.; Challacombe, M.; Gill, P. M. W.; Johnson, B. G.; Chen, W.; Wong, M. W.; Andres, J. L.; Head-Gordon, M.; Replogle, E. S.; Pople, J. A. *Gaussian 98*, revision A.7; Gaussian, Inc.: Pittsburgh, PA, 1998.

(9) Reed, A. E.; Curtiss, L. A.; Weinhold, F. *Chem. Rev*. **1988**, *88*, 899.

(10) Boys, S. F.; Bernandi, F. *Mol. Phys*. **1970**, *19*, 553.

(11) Cabaliero − Lago, E. M.; Rios, M. A. *Chem. Phys*. **2000**, *254*, 11.

(12) Dimitrova, Y. *J. Mol. Struct*. **1995**, *343*, 25.

(13) Ayala, R.; Martinez, J. M.; Pappalardo, R. R.; Marcos, E. S. *J. Phys. Chem. A* **2000**, *104*, 2799.

(14) Hobza, P.; Havalas, Z. *Chem. Rev*. **2000**, *100*, 4253.